

# Lithium–Niobate Ferroelectric Material Obtained by Glass Crystallization

M. Todorović<sup>a</sup> & Lj. Radonjić<sup>b</sup>

<sup>a</sup>Faculty of Technology and Metallurgy, Belgrade University, Karnegijeva 4, 11000, Belgrade, Yugoslavia

<sup>b</sup>Faculty of Technology, University Novi Sad, Bulevar cara Lazara 1, 21000, Novi Sad, Yugoslavia

(Received 2 July 1995; accepted 4 October 1995)

**Abstract:** Ferroelectric lithium–niobate ( $\text{LiNbO}_3$ ) crystals obtained by glass crystallization were investigated. The glass samples of the composition within the system  $\text{LiNbO}_3\text{--SiO}_2\text{--Al}_2\text{O}_3$  were prepared by melting process and then subjected to crystallization by the heat-treatment method, at the appropriate temperatures, between 500 and 900°C and for the times 10–60 min. Transparent glass-ceramics could be obtained. It was shown that in the investigated system the Layton's criterion  $B/N > 1$  has significant influence for the glass-ceramic's transparency. The  $\text{Al}_2\text{O}_3$ -content, according to Kokubo's suggestion, is not the primary factor for high nucleation rate in this system.

IR absorption spectroscopy analysis of the prepared glass samples shows that in the obtained glass network, which consists of  $\text{SiO}_4$ -tetrahedra and  $\text{NbO}_6$ -octahedra, the lithium ions are situated in the holes of the network closer to  $\text{NbO}_6$ -octahedra than  $\text{SiO}_4$ -tetrahedra.

XRD analysis of the crystallized glass samples shows that phase separation precedes the nucleation of  $\text{LiNbO}_3$  in glass matrix. At 650°C, crystallization of  $\text{LiNbO}_3$  is the most intensive.

SEM analysis of the crystallized glass samples shows that the crystal size of  $\text{LiNbO}_3$  increases with the increasing temperature and time of the heat-treatment. It could be seen that crystal growth is not classical, it takes place by nuclei coalescence within the clusters.

The measured values of dielectric constant and refractive index, at a frequency of 1 kHz and at room temperature, are between those of the noncrystallized parent glass and the pure  $\text{LiNbO}_3$  crystal.

It could be concluded that the obtained transparent glass-ceramics based on  $\text{LiNbO}_3$  crystals can be considered as a good ferroelectric material. © 1996 Elsevier Science Limited and Techna S.r.l.

## 1 INTRODUCTION

Lithium–niobate as a single crystal material is a very important ferroelectric material for application in optics and electronics because of its good ferroelectric properties, such as: large electro-optic effect, photorefractive effect, holographic effect<sup>1</sup> and so on. Very intensive investigations in this system have resulted in the development of many different techniques of  $\text{LiNbO}_3$  preparation and properties measurements, but  $\text{LiNbO}_3$  is still, until now, a great paradigm.<sup>2</sup>

However, lithium–niobate as a ferroelectric material can be prepared by the controlled glass crystallization process, as glass-ceramics,<sup>3–8</sup> starting

from the glasses with the large amount of the oxide, which are constituents of a ferroelectric phase and a low amount of glass-forming oxides.

Transparent ferroelectric glass-ceramics, as compared with single crystals and sintered ceramics, offer many advantages: dielectric constant is nearly independent of temperature; the properties can be considerably altered by varying the type of ferroelectric crystal and its size; and the material can be obtained relatively easily and cheaply.

One of the important properties required for the good ferroelectric glass-ceramics is high optical transparency. Generally, a glass-ceramic is transparent when: (1) its constituent crystal particles are so small in size that they produce no effective light

scattering of the visible spectrum, and (2) when the refractive indices of the glassy and crystal phases have very close values. For obtaining transparent ferroelectric glass-ceramics, the first condition must be satisfied, since the refractive index of ferroelectric crystals is usually much higher than that of the glassy matrix. For that reason, the nucleation rate of the crystal phase, in the glassy matrix, must be extremely high in order to release a small crystal size.

Literature data<sup>4-7</sup> show that two different reasons are responsible for the high transparency of glass-ceramics. One of them is Layton's B/N atomic ratio<sup>5</sup> where B is ferroelectric oxide content ( $\text{Nb}_2\text{O}_5$ ) and N is the total content of glass-forming oxides ( $\text{SiO}_2$  and  $\text{Al}_2\text{O}_3$ ). Another one is Ito *et al.*'s<sup>6,7</sup> suggestion that  $\text{Al}_2\text{O}_3$  content is much more important factor than B/N ratio.

For many years, the present authors investigated the glass crystallization in the system  $A_2\text{O}-B_2\text{O}_5-\text{SiO}_2-\text{Al}_2\text{O}_3$ , where A is the alkalis and B is Nb or Ta, in order to obtain the transparent glass-ceramics.<sup>9,10</sup> It was found that in some systems with Li-ion, Layton's B/N ratio determines the transparency and in other systems with Na- and K-ions, Layton's criterion doesn't hold, but rather the  $\text{Al}_2\text{O}_3$  content.

The purpose of this work is to present the obtained results of directed crystallization of  $\text{LiNbO}_3$ -ferroelectric crystals in glassy-matrix, in order to obtain transparent ferroelectric glass-ceramics. Discussion of the experimental results was based on the relationship between the glass-structure parameters (as are B/N ratio, and  $\text{Al}_2\text{O}_3$  content) and the microstructure (as are phase composition and crystal size). Besides, the microstructures (which are the results of the preparation procedure and mechanism of glass crystallization) are related to the obtained electrical and optical properties.

## 2 EXPERIMENT AND RESULTS

### 2.1 Glass preparation

In order to determine the glass-forming region in the investigated system, batch mixtures of various oxide compositions, shown in Table 1, were prepared from reagent grade  $\text{Li}_2\text{CO}_3$ ,  $\text{Nb}_2\text{O}_5$ ,  $\text{SiO}_2$  and  $\text{Al}_2\text{O}_3$ . They were melted in 30 g amounts in a platinum crucible, in a kanthal electric furnace, at 1300–1450°C for 1 h. The melts were poured on to a steel plate and immediately pressed into plates, approximately 1 mm thick. They were then quickly put into a preheated electric furnace, annealed at 500°C for 2–3 h and cooled with the furnace.

Table 1. Glass composition

Sample notation	Oxide content (mol%)				B/N <sup>*</sup> ratio	Appearance
	$\text{Li}_2\text{O}$	$\text{Nb}_2\text{O}_5$	$\text{SiO}_2$	$\text{Al}_2\text{O}_3$		
L-1	22.9	22.0	50.2	4.9	0.73	C
L-2	20.2	19.3	55.8	4.7	0.59	C
L-3	17.5	17.0	61.0	4.5	0.47	C
L-4	29.2	28.2	37.2	5.4	1.17	T
L-5	28.3	27.2	36.9	7.6	1.04	T
L-6	29.0	28.0	38.7	4.3	1.18	T
L-7	32.0	32.3	29.8	5.9	1.55	T
L-8	35.8	26.9	32.0	5.3	1.26	T

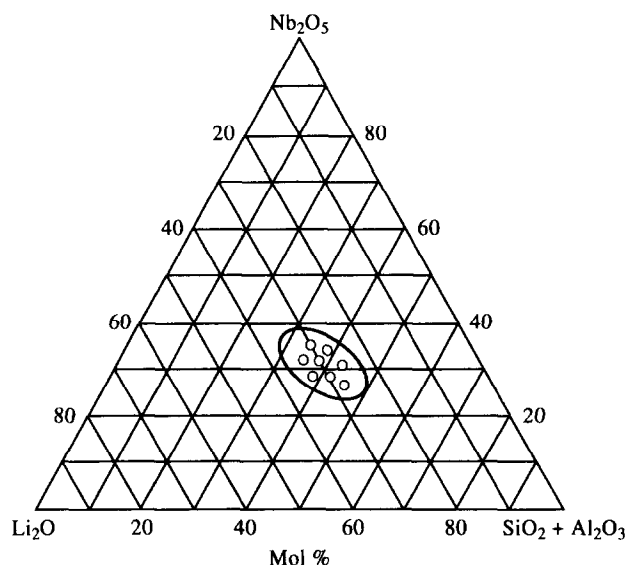


Fig. 1. Glass-forming region in the system  $\text{Li}_2\text{O}-\text{Nb}_2\text{O}_5-\text{SiO}_2-\text{Al}_2\text{O}_3$ .

Only some of the prepared glass samples were obtained as homogeneous, clear glasses, in a very limited composition region, given in Fig. 1 by enclosed solid line. Therefore, by observation with the naked eye, all the prepared glass samples were classified into two groups: transparent glass (T) and crystallized glass (C), as marked in Table 1.

### 2.2 Heat treatment of glass samples

The transparent glass samples, marked in Table 1 as L-4, were cut into slabs about 5×5×1 mm. They were put into platinum sheet and introduced into a preheated electric furnace at the appropriate temperature, kept at this temperature for some time and finally taken out from the furnace and allowed to cool in air. The transparency of the heat-treated samples was examined visually; 'transparent' means that letters placed beneath the samples could be read through the samples. In Fig. 2 is shown transparency of the heat-treated samples, L-4, at the various temperatures, for 10 min.

Heat-treated conditions, visual appearance and phase composition obtained by XRD and SEM analysis of the heat-treated samples, L-4, are given in Table 2. Sample notation is as follows: L denotes

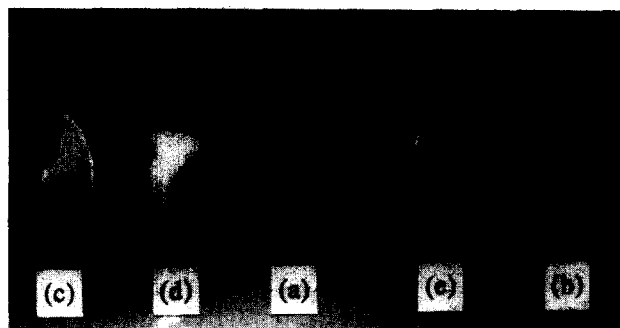


**Fig. 2.** Transparency of the heat-treated glass samples, L-4, at various heat-treatment conditions: (a) phase separated glass samples at 610°C for 10 min.; (b) crystallized at 620°C for 10 min.; (c) crystallized at 650°C for 10 min.; (d) crystallized at 900°C for 10 min.; and (e) crystallized at 650°C for 1 h.

**Table 2.** Heat-treatment conditions, visual appearance and phase composition of the sample L-4

Sample notation	Temperature (°C)	Time (min)	Appearance and phase composition of the heat-treated samples
L-4/A	500–600	10	transparent, glassy-phase
L-4/B	610	10	transparent, phase separation on the scale 20–50 nm
L-4/C	620	10	transparent, nucleation of LiNbO <sub>3</sub> , 50–150 nm
L-4/D	650	10	transparent, crystallization of LiNbO <sub>3</sub> , 150–350 nm
L-4/E	650	30–60	opaque, crystallization of LiNbO <sub>3</sub> , 800–1000 nm
L-4/F	700–900	10	opaque, crystallization of LiNbO <sub>3</sub> , 800–1000 nm

glass system with lithium, arabic number denotes the glass composition given in Table 1 and additional letter denotes heat-treatment conditions.

### 2.3 IR absorption spectroscopy analysis

Evaluation of the glass structure was estimated by infrared (IR) spectroscopy (Perkin-Elmer 521), using KBr disc method. In Fig. 3 are given IR absorption spectra of glass samples before heat-treatment (sample L-4) and after crystallization (sample L-4/D).

### 2.4 X-ray diffraction and scanning electron microscopy analysis

The heat-treated samples were subjected to the powder X-ray diffraction, XRD, analysis. In Fig. 4 are given X-ray diffraction patterns of the heat-treated samples, L-4, at: 610, 620 and 650°C, for 10 min.

Scanning electron microscopy, SEM, analysis (JEOL 45) was used for microstructure investigation. Fresh fractured surfaces of the heat-treated

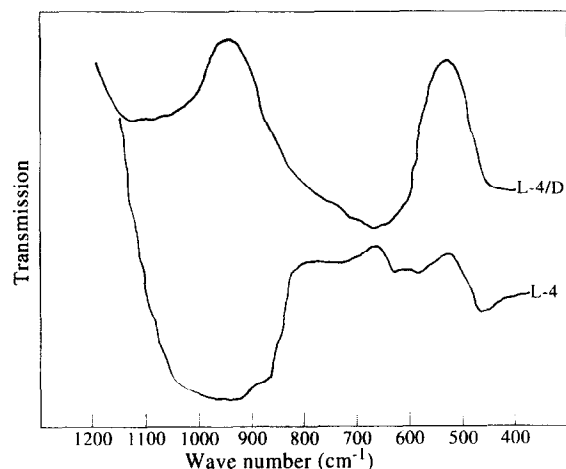


**Fig. 3.** Infrared absorption spectra of glass sample L-4 before crystallization and L-4/D after crystallization at 650°C for 10 min.

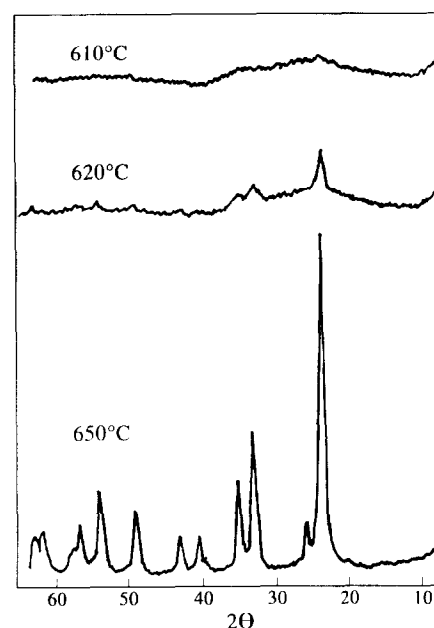


**Fig. 4.** X-ray diffraction patterns of the heat-treated glass samples L-4 at 610, 620 and 650°C for 10 min.

samples etched with 3% hydrofluoric acid, for 30 s, were used for SEM observation. In Fig. 5 are given electron micrographs of the heat-treated samples, L-4, at: 610, 620 and 650°C, for 10 min.

### 2.5 Electrical and optical properties

The permeativity of the heat-treated samples, which were polished on both sides and silver painted to form electrodes, was measured on 4194 A Impedance Analyser, Hewlet Packard, at a frequency of 1 kHz and at room temperature. Refractive index of the crystallized samples was measured on the goniometer, Carl Zeiss Jena, at room temperature.

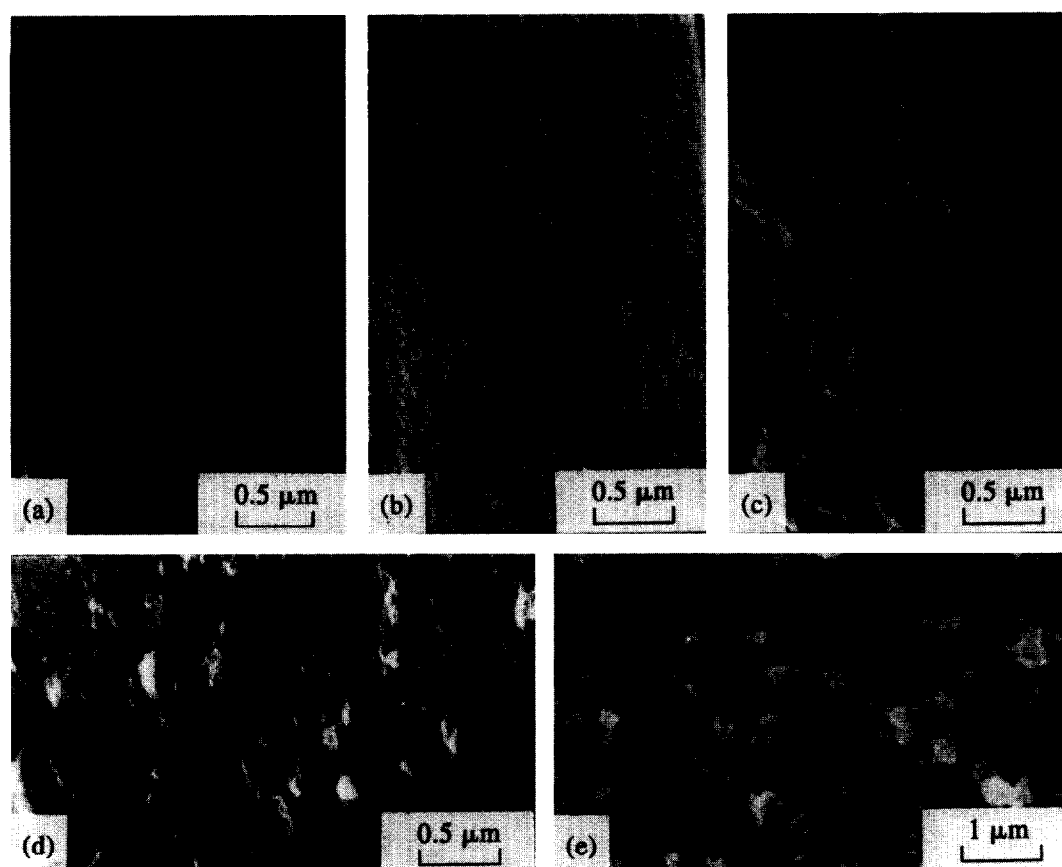


Fig. 5. Electron micrographs of the heat-treated glass samples L-4 at (a) 610, (b) 620 and (c) 650°C for 10 min., (d) 650°C for 30 min., and (e) 650°C for 60 min.

### 3 DISCUSSION OF RESULTS

#### 3.1 Glass preparation

Glasses containing a low content of network-formers are very fluid and crystallize rapidly during cooling at temperatures close to the liquidus. A very rapid cooling rate from the liquid- to the glassy-state is necessary to prevent crystallization. Therefore, these glasses could be prepared only in a very narrow composition region. The glass composition and the region in which homogeneous transparent glasses were obtained are given in Table 1 and Fig. 1. It could be seen that the stable glasses were obtained for the ratio  $B/N > 1$  and the  $Li_2O$  content greater than 25 mol%, which is in agreement with the Layton's criterion. However, the  $Al_2O_3$  content does not have the primary role in the glass-forming region.

Discussion of the IR absorption spectra are based on Kokubo's<sup>12-14</sup> hypothesis of glass-structure in these systems (a random network of  $SiO_4$ -tetrahedra and  $NbO_6$ -octahedra with the alkalis being situated in some holes of the network), and using the typical absorption bands of pure silica: stretching vibration band, S, at  $1080\text{ cm}^{-1}$ , deformation vibration band, D, at  $455\text{ cm}^{-1}$  and ring

vibration band, R, at  $800\text{ cm}^{-1}$ .<sup>15,16</sup> The absorption bands between  $900$  and  $650\text{ cm}^{-1}$  are attributed to the Nb-O vibration bond<sup>17</sup> and the tetrahedrally coordinated alumina.<sup>12</sup>

At approximately  $950\text{ cm}^{-1}$  appears an absorption band, arising from the silica non-bridging oxygen in the alkali-silicate glasses. Addition of alkali ions into a silica glass results in the shifting of S, D and R bands to the lower wave numbers and they become more shallow.

Figure 3 shows that S- and D-bands in the non-crystallized glass-samples L-4 are very steep. The band attributed to the silica nonbridging oxygen is rather separated from the S-band. From these results it was concluded<sup>10</sup> that lithium-ions are situated closer to the  $NbO_6$ -octahedra than  $SiO_4$ -tetrahedra in the glass network.

#### 3.2 Glass crystallization

IR absorption spectra (Fig. 3) show that the S- and D-bands of the crystallized glass samples (L-4/D, Fig. 3) are not shifted and that they appear at approximately  $1080$  and  $455\text{ cm}^{-1}$ , respectively, which is in agreement with the fact that alkali ions are now bonded in the ferroelectric crystal  $LiNbO_3$ .

From the XRD and SEM analysis (Figs 4 and 5) could be seen that at 610°C, the phase separation on the scale 20–50 nm occurred. At 620°C, LiNbO<sub>3</sub> nuclei appeared and LiNbO<sub>3</sub> intensively crystallized at 650°C on larger scale, 150–350 nm. It could be seen that crystal growth is not classical, it is rather abnormal, by nuclei coalescence in the clusters.<sup>5,11</sup> At the higher temperatures of 700–900°C for 10 min, and at the lower crystallization temperature of 650°C for the longer times of heat-treatment, 20–60 min., opaque glass-ceramics with LiNbO<sub>3</sub> crystals about 800–1000 nm in size were obtained (Table 2).

Mechanism of nucleation is in good agreement with the results reported by Layton and Herzog.<sup>5</sup> Phase separation appearance is significant for high nucleation rate without substantial grain growth. Phase separation could originate from micro-heterogenetics forming part of the glass structure, as NbO<sub>6</sub>-octahedra. Their number increase with increasing B/N ratio. Further grain growth takes place by coalescence of crystalline particles within clusters without a change in the concentration of the respective phases.

Also, Ito *et al.*<sup>6,7</sup> concluded that in the investigated system, LiTaO<sub>3</sub>–SiO<sub>2</sub>–Al<sub>2</sub>O<sub>3</sub>, nucleation of crystal phase in glassy-matrix is much easier in the phase separated regions rich with components making crystal phase than in original homogeneous glass, since: (a) the change of Gibbs energy of the bulk transformation of glass into crystal is higher; (b) surface energy of the crystal–glass interface is lower; and (c) the activation energy of atomic rearrangement for the nucleation is lower in the phase-separated glass than in the parent glass. However, these authors believe that for phase separation appearance the Al<sub>2</sub>O<sub>3</sub> content in glasses is a much more important factor than B/N ratio. They assumed that sharp competition between the Al<sup>3+</sup> and Ta<sup>3+</sup> ions in the investigated LiTaO<sub>3</sub>–SiO<sub>2</sub>–Al<sub>2</sub>O<sub>3</sub> system, in the Li<sub>2</sub>O-rich phase to occupying oxygen ions make this phase unstable. The Al<sup>3+</sup> ions are forced to utilize the oxygen already binding two NbO<sub>6</sub>-octahedra in the glass network, forming structural units, called by Lacy<sup>18</sup> as ‘triclusters’. The units also form structurally more inflexible regions in the glass network, which allowed phase separation appearance during the heat-treatment, i.e. they would be nucleation sites for crystallization and thus enhance the rate of nucleation of the LiTaO<sub>3</sub> crystals.

However, our experimental results rather follow Layton’s criterion than Ito’s suggestion. The Al<sub>2</sub>O<sub>3</sub> content in glass composition probably affects the mechanism of crystallization, besides B/N ratio. Relatively easy nucleation of LiNbO<sub>3</sub> in

**Table 3. Experimentally determined values of dielectric constant ( $\epsilon$ ), refractive index ( $n$ ), crystal size ( $D$ ) and volume content of LiNbO<sub>3</sub> phase ( $W$ ) of the crystallized samples L-4, at 650°C for 10 min**

Sample	Properties			
	$\epsilon$	$n$	$D$ (nm)	$W$ (% vol.)
L-4/D	155–185	1.84–1.93	150–350	45–50

comparison to other investigated systems such as NaNbO<sub>3</sub> and KNbO<sub>3</sub><sup>9,10</sup>, which manifested in the lowest phase-separation and nucleation temperature, could be explained using the results obtained by IR absorption spectroscopy analysis, i.e. with the conclusion that Li-ions are located in the glass-network closer to NbO<sub>6</sub>-octahedra than to SiO<sub>4</sub>-tetrahedra.<sup>10</sup>

### 3.3 Electrical and optical properties

In Table 3 are given experimentally determined values of dielectric constant,  $\epsilon$ , refractive index,  $n$ , together with average crystal size,  $D$ , and volume content of LiNbO<sub>3</sub> phase in the glassy-matrix,  $W$ , of the crystallized glass samples L-4, heat-treated at 650°C for 10 min.

Besides, the dielectric constant and refractive index were calculated for the glass sample L-4, by Schott’s additive formula.<sup>20</sup> These values are 20 and 1.80, respectively. From the literature data<sup>21</sup> are found that pure LiNbO<sub>3</sub> crystal-phase has  $\epsilon > 1000$  and  $n = 2.2$ . It could be seen that dielectric constant and refractive index increase during crystallization and they are in the intervals between values of parent glass and pure LiNbO<sub>3</sub> crystal.

Also, dielectric constant of the LiNbO<sub>3</sub> crystal-phase in the obtained glass-ceramics is calculated by Niesel’s approximate formula.<sup>19</sup> Using the experimentally obtained values for dielectric constants of glass-ceramics, it was found that pure LiNbO<sub>3</sub> crystal-phase has dielectric constants between 900 and 1000.

## 4 CONCLUSION

In the investigated Li<sub>2</sub>O–Nb<sub>2</sub>O<sub>5</sub>–SiO<sub>2</sub>–Al<sub>2</sub>O<sub>3</sub> system were synthesized homogeneous transparent glass samples, by melting process, only in a very narrow composition range, for the ratio B/N > 1.

IR absorption spectra show that lithium-ions are located in the glass network closer to NbO<sub>6</sub>-octahedra than to SiO<sub>4</sub>-tetrahedra, which enables nucleation of LiNbO<sub>3</sub> crystals during heat-treatment relatively easily. The mechanism of crystallization of LiNbO<sub>3</sub> in glassy-matrix is based on phase-separation of

glass, which is followed by nucleation of crystal phase. Crystal growth is not classical, but rather abnormal, since it takes place by coalescence of nuclei of  $\text{LiNbO}_3$  forming the clusters.

Layton's B/N ratio has significant influence for the glass-ceramics' transparency. The  $\text{Al}_2\text{O}_3$  content is not the primary factor for high nucleation rate in this system.

Electrical and optical properties of crystalline phases are related to the microstructure features which are results of the glass composition and heat-treatment conditions. The measured values of dielectric constant and refractive index show that the obtained transparent glass-ceramics, based on  $\text{LiNbO}_3$  crystals, can be considered as a good ferroelectric material.

## REFERENCES

1. MAGNUSSON, R. & GAYLORD, T. K., *Appl. Opt.*, **13** (1974) 1545.
2. GUNTER, P., *Electro-optic and Photorefractive Materials*. Springer-Verlag, Berlin, 1986.
3. BEALL, G. H., US Patent No. 3 573 939, 1971.
4. HERZOG, A., *J. Am. Ceram. Soc.*, **47** (1964) 107.
5. LAYTON, M. M. & HERZOG, A., *Glass Technol.*, **10** (1969) 50.
6. ITO, S., KOKUBO, T. & TASHIRO, M., *Bull. Inst. Chem. Res.*, **54** (1978) 307.
7. ITO, S., KOKUBO, T. & TASHIRO, M., *Am. Ceram. Soc. Bull.*, **58** (1979) 591.
8. BEALL, G. H. & DUKE, D. A., *J. Mater. Sci.*, **4** (1969) 340.
9. TODOROVIĆ, M. & RADONJIĆ, Lj., In *High Tech. Ceramics*, ed. P. Vincenzini. Elsevier Science Publishers, Amsterdam, The Netherlands, 1987, p. 2106.
10. TODOROVIĆ, M., RADONJIĆ, Lj. & NIKOLIĆ, Lj., *J. Serb. Chem. Soc.*, **59** (1994) 229.
11. TODOROVIĆ, M., RADONJIĆ, Lj. & DUMIĆ, J., *Mater. Sci. Forum*, **94-96** (1992) 891.
12. TARTE, P. W., *Physics of Non-Crystalline Solids*, ed. J. A. Prins. North Holland, Amsterdam, 1965, p. 549.
13. KOKUBO, T., NISHIMURA, M. & TASHIRO, M., *J. Non-Cryst. Solids*, **15** (1974) 329.
14. KOKUBO, T., NISHIMURA, M. & TASHIRO, M., *J. Non-Cryst. Solids*, **22** (1976) 125.
15. HENCH, L. L., *J. Non-Cryst. Solids*, **19** (1975) 27.
16. PRASSAS, M., PHALIPPON, J., HENCH, L. L. & ZARZYCKI, J., *J. Non-Cryst. Solids*, **48** (1982) 79.
17. SARJEANT, P. T. & ROY, R., *J. Am. Ceram. Soc.*, **50** (1967) 500.
18. LACY, E. D., *Phys. Chem. Glasses*, **4** (1963) 234.
19. NIESEL, W., *Ann. Physik*, **10** (1952) 330.
20. VUKULEV, G. V. & PIVEN, I., *Zadaènik po himii kremnia i fizièeskoi himii silikatov*. Višaja škola, Moskva, 1971, pp. 140-70.
21. GMELIN, L., *Gmelins handbuch der anorganischen chemie*, Achte völlig neu bearbeitete Auflage. Springer Verlag, Berlin, Heidelberg, New York, 1974, Niob, Teil B4, pp. 30, 107 and 148.